Green Chemistry

PAPER

View Article Online
View Journal

Cite this: DOI: 10.1039/d5gc02409a

The acetate anion promotes hydrolysis of poly(ethylene terephthalate) in ionic liquid–water mixtures

Maariyah Y. Suleman,†[a] Harriet L. Judah, †[a] Panagiotis Bexis, [a] Paul Fennell,[b] Jason P. Hallett [b] and Agnieszka Brandt-Talbot *[a]

A circular plastic economy reduces raw material consumption and discourages pollution. Chemical recycling upgrades the quality of recyclate and is a complementary approach to thermomechanical recycling of plastic waste. This study investigated the use of aprotic and protic ionic liquids (ILs) as solvents for chemical recycling by the hydrolysis of the most common polyester plastic, poly(ethylene terephthalate) (PET). Combinations of three types of cations (aprotic 1-alkyl-3-methylimidazolium, protic 1-methylimidazolium and protic 1,5-biazocyclo-[4.3.0]non-5-enium) combined with a range of anions (acetate, chloride, methanesulfonate, hydrogen sulfate, methyl sulfate, trifluoromethanesulfonate and chlorozincate) were used to hydrolyse PET in the presence of 15 wt% water as the co-solvent and reagent. PET conversion under the screening conditions (180 °C, 3 h, 5% PET loading) varied between 1 and 100%, with ILs containing the acetate anion enabling >97% PET conversion irrespective of the cation. Acidification with aqueous HCl recovered crude crystallised terephthalic acid (TPA). Significant crude yields (46–93%) were only observed for the acetate ILs. The purity of the crude TPA was 34–98%, with 1-ethy-3-methylimidazolium acetate, [C_2C_1im][OAc], and 1-methylimidazolium acetate, [C_1Him][OAc], yielding more and purer TPA than 1,5-biazocyclo-[4.3.0]non-5-enium acetate, [DBNH][OAc]. TPA solubility, PET conversion and TPA yield generally correlated well with increasing pK_a and higher hydrogen bond acceptor strength of the IL anion, suggesting that the depolymerisation mechanism in the acetate IL water mixtures is base catalysed. The screening identifies aqueous mixtures of the (pseudo)-protic IL [C_1Him][OAc] as promising catalytic solvent component for the chemical recycling of PET at an industrially feasible temperature, due to high isolated TPA yields and purity achieved at a low solvent cost ($1.74–2.15 per kg). However, an effective separation approach for the monomers TPA and ethylene glycol from the solvent remains to be developed.

Received 14th May 2025,
Accepted 7th August 2025

DOI: 10.1039/d5gc02409a

rsc.li/greenchem

Green foundation

1. This work advances green chemistry by identifying water-containing ionic liquids, especially the low-cost protic ionic liquids, such as 1-methylimidazolium acetate, [C_1Him][OAc], as effective media for PET depolymerisation. Using the solvent mixture offers milder reaction conditions compared to conventional methods. This approach supports circular economy goals by enabling chemical recycling of plastic waste.

2. By employing [C_1Him][OAc] with 15 wt% water, the study achieved 98.5% PET conversion and 82.4% crude TPA yield with 77.8% purity using moderate hydrolysis conditions (180 °C, 3 h). The IL is easy to prepare and low-cost (~$2 per kg), which is >10 times lower than the cost of the analogous aprotic ionic liquid solvent. The study also introduced chromatographic purity analysis, improving the accuracy of performance evaluation over purely gravimetric methods.

3. Future work should develop monomer recovery methods that avoid acid addition to reduce waste generation during monomer isolation and enable IL reuse. Research into process intensification (higher loading), and application to mixed and degraded plastic waste will enhance the environmental and practical impact of this method.

Introduction

PET is a commodity plastic that is widely used in applications such as packaging, construction, textiles and electronics,[1,2] accounting for 6.2% of global plastic production.[3,4] The European PET bottle recycling rate was 50% in 2022, which

[a]Department of Chemistry, Imperial College London, London, W12 0BZ, UK. E-mail: agi@imperial.ac.uk
[b]Department of Chemical Engineering, Imperial College London, London, SW7 2AZ, UK
†These authors contributed equally to this work.

was achieved through thermomechanical recycling, consisting of shredding waste PET to produce flakes that can be melted and re-extruded into recycled plastic pellets. Thermomechanical recycling is a well-developed technology; however, the recycled plastic typically has degraded material properties. For example, it is coloured or has reduced mechanical strength, caused by lower molecular weight and contamination with other polymers and materials.[5,6] As a result, mechanically recycled PET from bottles and food packaging is often used in applications with less stringent specifications for mechanical strength and transparency, such as polyester textiles, while textile PET remain unrecycled.[7] To encourage the use of recycled PET in food packaging and make coloured polyester textiles recyclable, methods to purify and upgrade PET-containing waste are required.[8]

Chemical plastic recycling encompasses a variety of methods that employ heat or chemical agents to separate additives from the polymer or to break the chemical bonds in the polymer, which recovers chemical feedstocks, purified oligomers or monomers.[9] Biological plastic recycling employs microorganisms or enzymes to break chemical bonds in polymers to facilitate recycling at the oligomer or monomer level.[10] PET is a condensation polymer and can be chemically recycled by cleaving the ester bonds, typically using a solvent containing nucleophiles such as water, glycols, alcohols, and amines, yielding a range of depolymerisation products (Fig. 1).[6,9,11–13] Challenges for chemical recycling *via* depolymerisation include avoiding the generation of by-products and chemical waste, and minimising the energy requirement for depolymerisation and monomer recovery.[14] PET is sparingly soluble in most solvents due to its high molar weight and crystallinity.[15] As a result, PET is typically depolymerised at the solid–liquid interface, including for approaches that employ ILs.[16–18]

Glycolysis of PET with ethylene glycol (EG) as the monomer, solvent and nucleophile is the most investigated approach, generating solubilised bis(2-hydroxyethyl) terephthalate (BHET) and EG. However, glycolysis faces challenges during purification, such as slow crystallisation of crude BHET at low temperatures, which requires cooling to 0–10 °C for up to 24 hours.[19,20] Recently, depolymerisation of PET in anhydrous acetic acid has been reported as an approach called acetolysis, yielding TPA and acetylated EG after evaporating the solvent.[13] While acetolysis results in rapid crystallisation of TPA, it requires anhydrous conditions and high temperatures (>280 °C).[13]

The depolymerisation of PET using water as the nucleophile (hydrolysis) is attractive, as it is a direct reversal of the industrial PET production method (Fig. 1). However, without a suitable catalyst, high temperatures and pressures or long reaction times are required to achieve depolymerisation.[21] Catalysts for PET hydrolysis can be inorganic and organic hydroxides, Lewis acids, ILs and deep eutectic solvents. PET hydrolysis has been carried out using aqueous solutions of sodium hydroxide (NaOH) at low temperatures of 50–80 °C, yielding crystallised TPA.[22] The TPA can only be isolated after reducing the pH by adding HCl or H_2SO_4 to protonate sodium terephthalate, which creates salt waste (NaCl or Na_2SO_4). Enzymes are effective at hydrolysing PET at low temperatures (55 °C), but reaction times are long (4 days) and addition of acid is required to precipitate the TPA.[23] Recently, PET was hydrolysed at 80–120 °C within 1 h using mixtures of iron salt hydrates

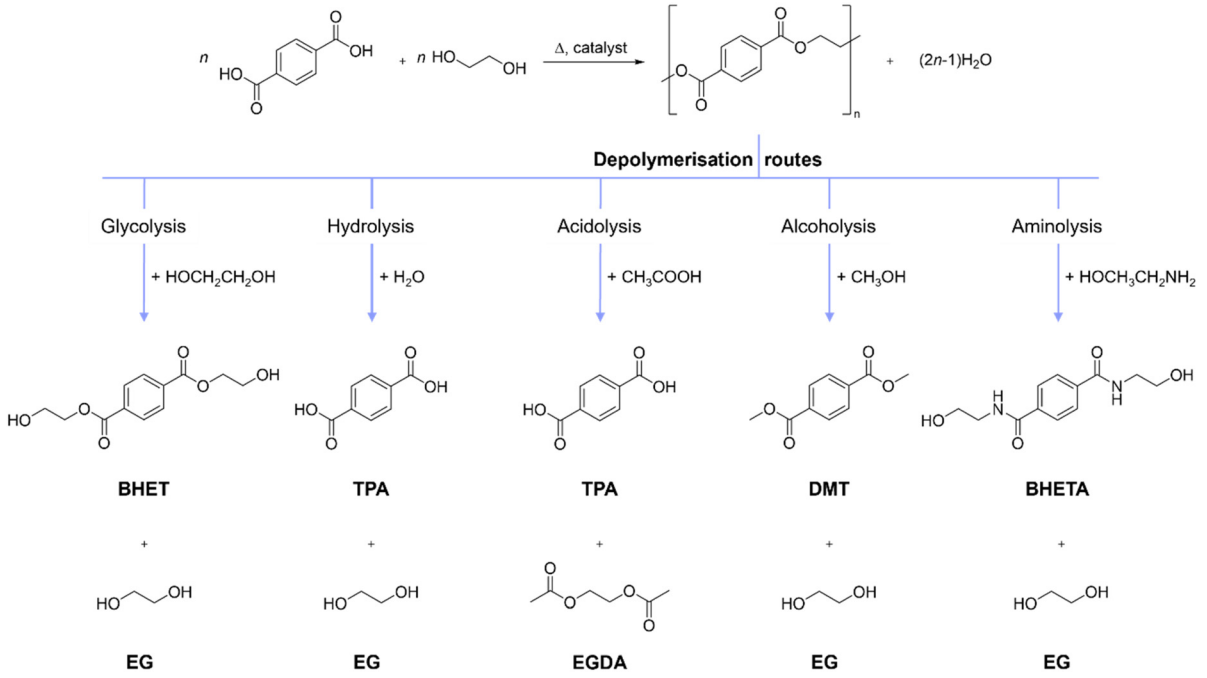

Fig. 1 Industrial production of PET and depolymerisation routes using various nucleophiles which produce terephthalic acid, bis(2-hydroxyethyl) terephthalate, dimethyl terephthalate, bis(2-hydroxyethyl) terephthalamide, ethylene glycol (EG) or ethylene glycol diacetate (EGDA).

and organic sulfonic acids, achieving PET conversion and an isolated crude TPA yield up to 100% and 96.4%, respectively. TPA precipitation occurred without the need to adjust the pH, instead, with water used as an anti-solvent. However, the crude TPA was bright yellow.[24]

ILs have been used as catalysts or catalytic solvents for PET depolymerisation, with IL-assisted glycolysis being the most commonly reported approach. The IL is used as a catalyst (approx. 5 wt% loading relative to EG) to accelerate the reaction or to replace the inorganic Lewis acidic catalyst, $Zn(OAc)_2$.[16,25–27] A number of protic ILs have been reported for PET glycolysis, for example, triazabicylodecanium methanesulfonate, [TBD][CH_3SO_3],[28] 1,5-diazabicyclo[4.3.0]non-5-enium 4-methylphenoxide, [DBNH][4-CH_3PhO],[27] 1,8-diazabicyclo [5.4.0]undec-7-enium imidazolate, [HDBU][Im],[29] 1,5,7-triazabicyclo[4.4.0]dec-5-enium acetate, [TBD][OAc],[30] and 2-hydroxyethyl ammonium acetate, [2-HEAA][OAc],[31] with complete PET conversion and BHET yields of at least 85%.

IL-assisted hydrolysis of PET has been less commonly reported. Hydrolysis of PET (polyester) fibre employing mixtures of 1-butyl-3-methylimidazolium hydrogen sulfate, [C_4C_1im][HSO_4], or 1-methylimidazolium hydrogen sulfate, [C_1Him][HSO_4], with 40–60 wt% water was demonstrated,[32] with PET conversion up to 80% at 185–195 °C after 2.5–3.5 h, while TPA yield and purity were not quantified. 1-Butyl-3-methylimidazolium chloride, [C_4C_1im]Cl, accelerated PET textile hydrolysis as 5% additive in aqueous and methanolic solutions of sodium hydroxide.[33] Choline lysinate, [Ch][Lys], enabled PET hydrolysis after 2 h at 180 °C, achieving 55% conversion and 56% un-isolated TPA yield.[34] Hydrolysis of PET in aqueous choline phosphate, $[Ch]_3[PO_4]$, was employed at 120 °C, yielding crude crystallised TPA after 3 h upon acidification, with the TPA yield not reported.[35] Liu *et al.* used a mixture of [C_4C_1im]Cl and 1-methyl-3-(3-sulfopropyl)-imidazolium hydrogen sulfate, [HSO_3-pmim][HSO_4], and 40 wt% water to hydrolyse PET at 170 °C for 4.5 h, reporting 89% crude isolated TPA yield after adding acid.[36] A 94% isolated TPA yield was reported for 1-(3-propylsulfonic)-3-methylimidazolium chloride, [HSO_3-pmim]Cl, mixed with 75 wt% water at 210 °C after 24 h, also employing acidification to isolate the TPA.[37] PET hydrolysis was reported in the presence of "switchable ILs" generated from a range of amines, CO_2 and water in a pressure reactor, with a reaction temperature of 150 °C and a reaction time of 6–24 h achieving up to ≥99% TPA yield upon acidification.[38] Only small groups (2–6) of ILs were compared by individual studies.

The product purity is often not considered in studies that report isolated TPA yields, or methods are applied that assess product purity only qualitatively, such as differential scanning calorimetry, thermogravimetric analysis, X-ray diffraction, mass spectrometry, and spectroscopic techniques.[16,27] Acid–base titration was used to assess purity quantitatively;[13] however, it cannot distinguish TPA from acetic acid, 2-hydroxyethyl terephthalic acid (HETA), and other carboxylic acid impurities such as *p*-toluic acid and 4-carboxybenzaldehyde. While NMR spectroscopy can provide quantitative insights, chromatographic separation is superior in precision and accuracy, and should be used for quantitative assessment of product purity.

This study systematically investigated the influence of the IL structures (anion and cation) on PET conversion and TPA yield following PET hydrolysis, with over 20 IL compositions used and with a focus on easy-to-synthesise protic ILs, which are synthesised through a proton transfer from a Brønsted acid to an amine. The study also demonstrates that chromatographic quantification and NMR spectroscopy are important tools to correctly report TPA yield and monitor product purity and solvent stability.

Experimental

Materials

Reagents were used as received unless specified otherwise. PET beverage bottles were washed with deionised water and dried before cutting to 0.5 mm size particles (SM 2000, Retsch), followed by sieving through a 0.5 mm mesh. 1-Ethyl-3-methylimidazolium acetate, [C_2C_1im][OAc], (>95%, 0.48% H_2O) and 1-butyl-3-methylimidazolium chloride, [C_4C_1im]Cl, (>98%, ≤1.0% H_2O) were purchased from IoLiTec Technologies (Germany). 1-Ethyl-3-methylimidazolium hydrogen sulfate, [C_2C_1im][HSO_4], (95%, 0.14% H_2O), 1-butyl-3-methylimidazolium methyl sulfate, [C_4C_1im][CH_3SO_4], (95%), deuterated dimethyl sulfoxide (DMSO-d_6, 99.96% atom% D), terephthalic acid (99%), 1-methylimidazole (99%), acetic acid (glacial, 99%), 1,3,5-trimethoxybenzene (≥99%) and HPLC-grade DMSO (≥99.7%) were purchased from Merck. Ethylene glycol (99.5%) was purchased from Acros Organics. 1,5-Diazabicyclo[4.3.0]non-5-ene (98%), trifluoromethanesulfonic acid (≥99%) and methanesulfonic acid (≥98%) were purchased from Fluorochem. Sulfuric acid (5 M) and hydrochloric acid (≥37%) were purchased from Honeywell Fluka. Zinc chloride ($ZnCl_2$, ≥98%) was purchased from Alfa-Aesar. Sodium hydroxide (NaOH pellets, 98.5–100%) was purchased from AnalaR Normapur.

NMR spectroscopy

NMR spectra were recorded on a Bruker 400 MHz spectrometer at room temperature and processed using MestreNova software version 12 (Mestrelab Research, S.L., Santiago de Compostela, Spain). Chemical shifts (δ) are reported in parts per million (ppm). All NMR spectra were recorded in DMSO-d_6.

Synthesis of protic ionic liquids

Equimolar amounts of acid and amine (unless otherwise specified) were charged into a round-bottom flask with a stir bar. The acid was added *via* dropwise addition through a dropping funnel. An ice bath was used to maintain the temperature below 5 °C. The mixture was stirred overnight at room temperature to ensure complete mixing. Deionised water was added as needed to produce ILs containing 15 wt% H_2O. [C_4C_1im]Cl, [C_4C_1im][$MeSO_4$], [DBNH][OAc], [DBNH][OAc] (1 : 2), [DBNH][OAc] (2 : 1), [DBNH][$MeSO_3$], [C_1Him][OTf] and [C_1Him][$MeSO_3$] were

solid at room temperature, so they were manually ground into powder and dried under vacuum before water was added. The water content of all synthesised ILs was adjusted to 15 wt%. If above this value, the water content was reduced using a rotary evaporator and measured using a volumetric Karl-Fischer titrator (Mettler Toledo titrator, EasyPlus Easy KFV). All ILs used in this work are shown in Fig. 2 and Table S1. The synthesised ILs were characterised with NMR spectroscopy and their detailed syntheses are described in the SI (Fig. S1–S12).

PET hydrolysis

0.100 g of PET powder and 2.0 g of IL–water mixtures (15 ± 0.5 wt% water) were added to a 15 mL pressure tube (Aceglass) and sealed with a Teflon cap and O-ring (silicon or FETFE), forming a suspension with 5% PET loading according to eqn (1), in which m_{PET}, m_{IL} and m_{water} are the weights of the components:

$$\text{PET loading}\,(\%) = \frac{m_{PET}}{m_{IL} + m_{water}} \times 100 \quad (1)$$

Samples were placed in a preheated oven (Binder ED 23, Binder GmbH) at the selected temperature (usually 180 °C) for a selected length of time. After hydrolysis, the pressure tube was cooled to room temperature for at least 30 min. If a solid residue was present, 2 M sodium hydroxide was added until pH 10–11 was reached to dissolve TPA, using pH strips for monitoring. The remaining residue was assumed to be PET and separated *via* vacuum filtration using a Buchner funnel and a Whatman™ 542 hardened ashless filter paper. The solid residue was washed with deionised water, dried in a vacuum oven at 60 °C for 24 h and the weight recorded. The weight was used to calculate PET conversion as follows (eqn (2)):

$$\text{Conversion}_{PET}\,(\%) = \frac{m_{PET_0} - m_{PET_1}}{m_{PET_0}} \times 100 \quad (2)$$

where m_{PET_1} is the weight of the residue (if present) and m_{PET_0} is the initial weight of the PET powder prior to hydrolysis.

To recover crude TPA, the filtrate was acidified with 37% aqueous HCl until pH 2–3 was reached (monitored using pH strips) and the solution became cloudy. The suspension was refrigerated (4 °C) for 24 h to complete precipitation, followed by vacuum filtration and washing with deionised water. The precipitate was dried in a vacuum oven for 24 h at 60 °C on the filter paper before recording the weight of isolated TPA. The crude TPA yield was calculated as follows (eqn (3)):

$$\text{Yield}_{\text{TPA crude}}\,(\text{wt}\%) = \frac{m_{TPA}/M_{TPA}}{m_{PET,0}/M_{PET}} \times 100 \quad (3)$$

where m_{TPA} is the weight of the TPA product isolated after acidification, $m_{PET,0}$ is the initial weight of PET added to the IL–water mixture. M_{TPA} and M_{PET} are the molar weights of TPA (166 g mol^{-1}) and the PET repeating unit (192 g mol^{-1}), respectively.

Determination of TPA purity in the crude product

The content of TPA in the crystallised product was determined using high performance liquid chromatography (HPLC) using a 1260 Infinity II Hybrid SFC/UHPLC (Agilent Technologies). The HPLC was equipped with an auto-sampler, a C-18 column (Raptor C18, 50 × 2.1 mm, 2.7 μm) and a UV-Vis diode array detector, with a wavelength of 254 nm used for detection. A gradient of acetonitrile and 0.1% formic acid (aq) was used as the mobile phase. HPLC samples were prepared in HPLC-grade DMSO using 5.1 mM 1,3,5-trimethoxybenzene (TMB) as the internal standard. Calibration curves were prepared using purchased commercial TPA (99% purity). Isolated crude TPA (4–6 mg) was dissolved in a solution of DMSO containing 5.1 mM TMB. The solution was filtered through a PTFE microfilter with a 0.2 μm pore size to remove undissolved impurities and dust particles prior to analysis. A calibration curve for TPA was prepared ranging from 0.2 mM to 7.5 mM, and the calculated mass of TPA in the sample, $m_{TPA,calc}$, was determined *via*

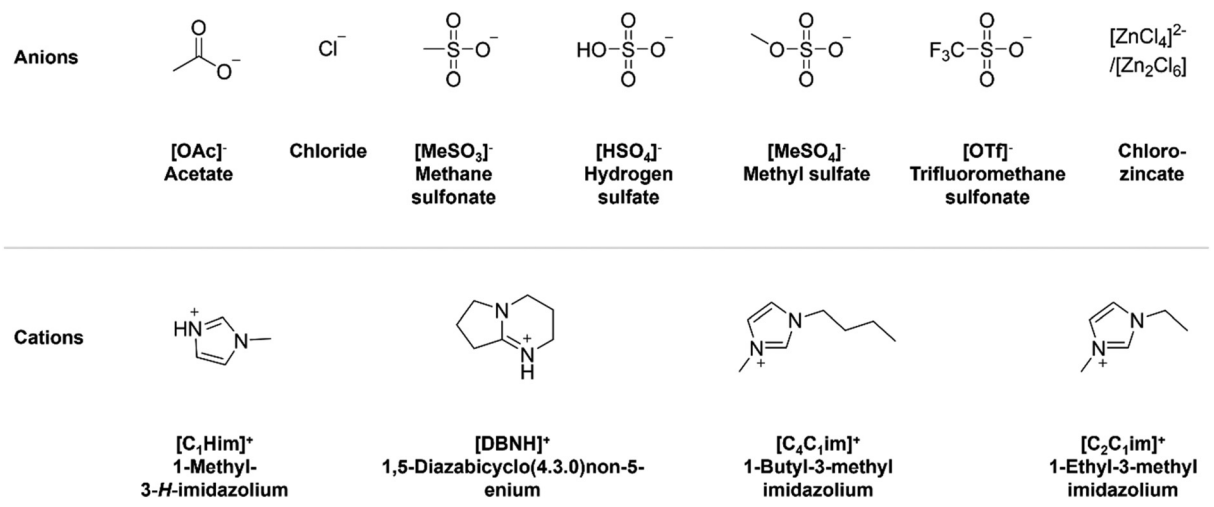

Fig. 2 Structures of anions and cations used to construct the protic and aprotic ILs employed in this work.

external calibration. TPA purity was calculated according to eqn (4):

$$\text{TPA mass purity (wt\%)} = \frac{m_{\text{TPA,calc}}}{m_{\text{TPA,sample}}} \times 100 \quad (4)$$

where $m_{\text{TPA,sample}}$ is the mass of crude TPA initially weighed to prepare the sample and $m_{\text{TPA,calc}}$ is the calculated mass of TPA content in the crude precipitate. Thus, the TPA purity is a weight percentage. TPA peak purity was also determined and compared to TPA mass purity. TPA peak purity was determined according to eqn (5):

$$\text{TPA peak purity (\%)} = \frac{\text{TPA peak area } (m\text{AU})}{\text{Total peak area } (m\text{AU})} \times 100 \quad (5)$$

where total peak area is the sum of all peak areas, excluding internal standard, TMB (t_R = 4.7 min). An exemplary calibration graph, chromatograms and more details on TPA purity determination can be found in the SI (Fig. S13–S21). Following determination of the crude TPA mass purity (wt%), the pure TPA yield could be determined using eqn (6):

$$\text{Pure TPA yield (wt\%)} = \frac{(m_{\text{TPA}}/M_{\text{TPA}}) \times \text{TPA purity}}{m_{\text{PET,0}}/M_{\text{PET}}} \times 100 \quad (6)$$

whereby the TPA purity used in the equation is specifically the TPA mass purity determined in accordance with eqn (4).

Monomer solubility screening

0.100 g of TPA mixed with 2.0 g of IL solution or solvent (water, acetic acid, 1-methylimidazole, or 1,5-diazabicyclo [4.3.0]non-5-ene) containing 15 wt% water was placed in a 15 mL pressure tube with a Teflon cap and silicon or FETFE O-ring. The tube was heated at 180 °C for 3 h in a pre-heated oven. The solutions were visually inspected while still in the oven to see if the TPA was solubilised, and once they had cooled down, a photograph was taken (in Fig. S22) and the qualitative observation was recorded.

Results and discussion

Ionic liquid selection and synthesis of protic ILs

Two imidazolium cations were selected, the aprotic 1,3-dialkylimidazolium cation type and the protic 1-methylimidazolium cation type (Fig. 2). ILs with an imidazolium cation are well studied in the literature and relatively stable when heated.[36,39,40] Due to the low pK_a of 1-methylimidazole (pK_a = 7.1),[41] an amidinium cation, 1,5-diazabicyclo[4.3.0]non-5-enium ($[DBNH]^+$), derived from an amine with a higher pK_a (pK_a = 12.8)[42] was also studied. The higher pK_a of the amidine nitrogen promotes preparation of protic ILs with a higher degree of proton transfer.[43] An unprecedented variety of anions were chosen which covers a wide range of hydrogen bond acceptor strengths.[39] In addition, an anion with Brønsted acidity ($[HSO_4]^-$) and one with the potential to generate Lewis acidic species ($[ZnCl_3]^-$) were included. The cation and anion selection was limited to ILs that are water miscible.

PET hydrolysis in ionic liquid–water mixtures

Protocol development with [C_2C_1im][OAc]. The AIL [C_2C_1im][OAc] was used to develop a screening protocol because high catalytic activity has been reported for PET glycolysis using this IL.[35] After surveying reaction conditions used in previously published studies on PET depolymerisation, 180 °C was chosen as the reaction temperature. PET hydrolysis at lower temperatures has been reported, but typically requires long reaction times.[44,45] The requirement for high temperature is assigned to the high crystallinity of PET and the ester bond being stabilised by a conjugated benzene ring. The 15 wt% water content represents a balance between retaining the IL as the dominant solvent component by mass, while ensuring that the IL–water mixture is liquid at room temperature and contains an excess of water (16 times more moles of water than PET ester linkages). The 5 wt% PET loading ensured sufficient product for accurate quantification with a microbalance while ensuring complete wetting of plastic particle surface and minimal impact of solid loading on conversion.

PET conversion was observed in the [C_2C_1im][OAc]–water mixture (Fig. 3) and depolymerisation was confirmed by detecting peaks for TPA and EG in the ^{1}H-NMR spectrum of the post-hydrolysis solution (Fig. S23a). The reaction time was varied between 0.5 h and 5.5 h at the screening temperature (Fig. 3a), showing that PET conversion reached 100% at around 2.5 h for the [C_2C_1im][OAc]–water mixture. The reaction temperature was also varied between 140 and 180 °C, with PET conversion decreasing with lower reaction temperature as expected (Fig. 3b). The screening experiments confirmed that 180 °C is an appropriate temperature for the 3 h reaction time.

Isolating the crude TPA product. To demonstrate the potential for isolating TPA from the reaction mixtures and focus on the screening, aqueous HCl was added, with pH 3 inducing precipitation. The filtration of the suspension was accompanied by washing with deionised water to afford a white or off-white precipitate, regardless of the colour of the IL–water mixture post-hydrolysis (Fig. S24). ^{1}H-NMR spectroscopic analysis confirmed that the isolated product was mostly TPA (Fig. 4). A detailed discussion of the crude TPA composition is presented below.

Interestingly, a lag was observed between PET conversion and TPA yield, the difference being more prominent at shorter reaction times and lower reaction temperatures (Fig. 3). A maximum crude TPA yield (92%) was observed at around 3.3 h, which occurred ~50 min after achieving full PET conversion. The lag suggests that intermediate depolymerisation products form which are soluble in dilute aqueous acid, potentially glycol terminated oligomers and BHET. A gradual drop in yield at longer times suggests that slower reactions may have affected the purity of the crude product; however, the product purity was not determined for this set of experiments.

Effect of solvent composition on hydrolytic PET conversion and TPA yield. Next, the group of selected ILs were employed

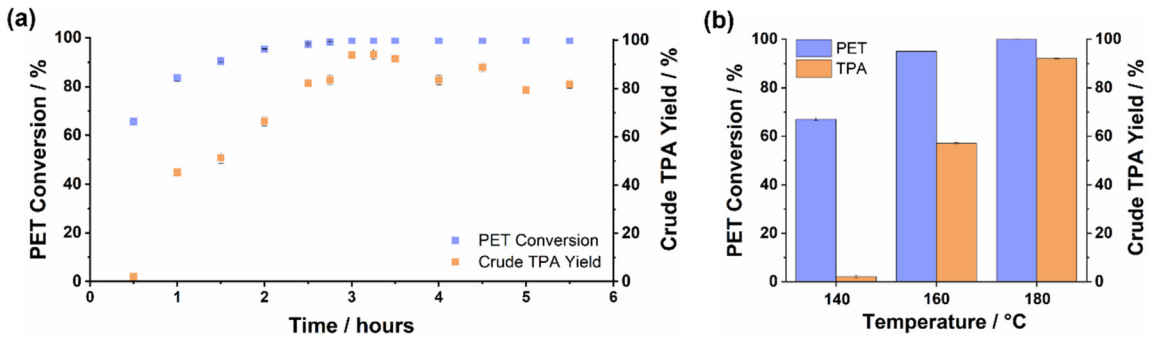

Fig. 3 PET hydrolysis in the benchmark IL, $[C_2C_1im][OAc]$, with 15 wt% water. (a) Conversion and isolated crude yield at 180 °C. (b) Impact of reaction temperature on PET conversion and isolated crude TPA yield at a reaction time of 3 h.

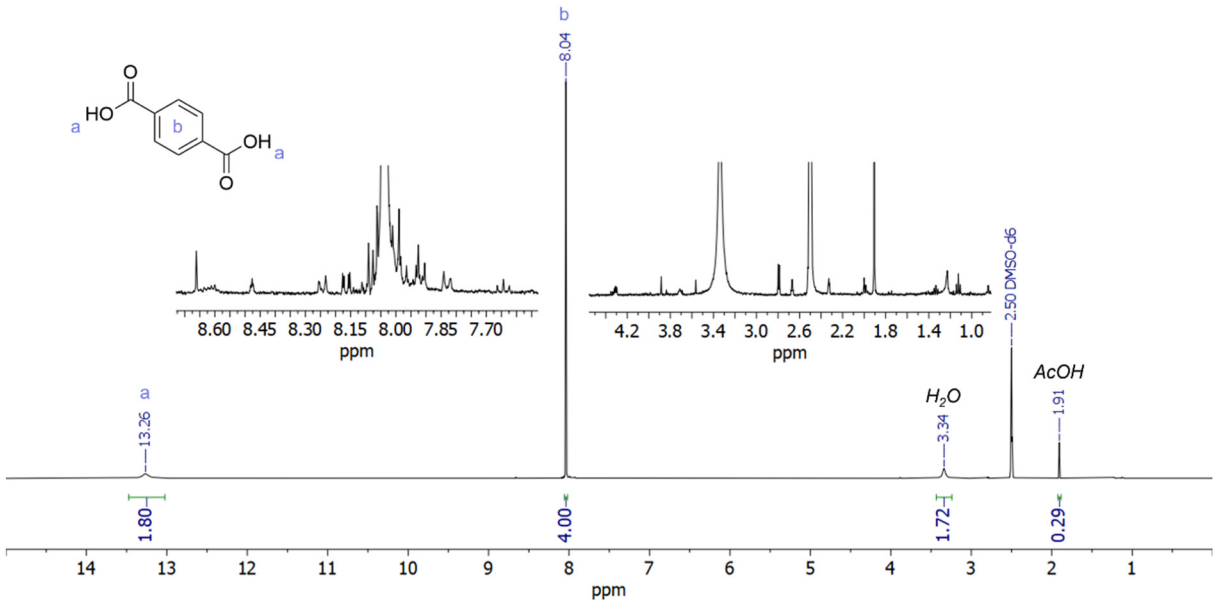

Fig. 4 ^{1}H-NMR spectrum of the isolated TPA product after PET depolymerisation with $[C_2C_1im][OAc]$ containing 15 wt% water, showing that the product was mainly TPA. Insets show additional peaks in the aromatic (7.5–8.8 ppm) and aliphatic (1–4.5 pm) regions of the spectrum. Reaction conditions: 3 h, 180 °C, 5 wt% PET loading. NMR solvent: DMSO-d_6.

using the screening conditions (180 °C, 3 h, 5% PET loading, 15 wt% water). A step was added that employed 1 M aqueous sodium hydroxide before filtration to ensure that all TPA was solubilised as sodium terephthalate, in case a solvent exhibited good conversion but low solubility for the monomer. Control experiments confirmed that raising the pH to 10–11 with 1 M sodium hydroxide did not cause measurable PET hydrolysis during the recovery. The unhydrolysed PET was separated by filtration and dried to determine PET conversion.

PET hydrolysis in acetate ILs. A strong dependency of PET conversion on the nature of the IL anion was observed (Table 1). All acetate ILs showed near-quantitative or quantitative conversion regardless of the cation, while the other IL–water mixtures converted 32% PET or less, demonstrating a step change in performance. Despite the high conversion observed for all acetate ILs, the isolated crude TPA yield varied substantially. The reference IL, $[C_2C_1im][OAc]$, generated the highest crude TPA yield (92%) during the screening, followed by $[C_1Him][OAc]$ (82%) and [DBNH][OAc] (47%) (Fig. 5). The monomers TPA and EG in acetate ILs were observed in ^{1}H-NMR spectra of the post-hydrolysis solution *via* a singlet peak at 3.4 ppm (EG) and one at 7.8–8.0 ppm (TPA) (Fig. S23). The study focused on isolation and purity of the larger of the two monomers (TPA) as an indicator of performance; however, attention must be paid to both TPA and EG to develop a viable recycling process.

Conversion and crude TPA yield were also determined for the amines used to generate the protic acetate ILs and for acetic acid (each containing 15 wt% water), and for deionised water as a control. PET conversion was observed for the three aqueous mixtures in the order diazabicyclo(4.3.0)non-5-ene (DBN) > 1-methylimidazole > acetic acid, but not in deionised

Table 1 PET conversion after hydrolysis at 180 °C for 3 h in ionic liquid and solvent water mixtures (15 wt%), while the TPA yield was determined gravimetrically following acidification and filtration

Solvent name	Abbreviation	PET conversion (%)	Isolated crude TPA yield (wt%)
1-Ethyl-3-methylimidazolium acetate	$[C_2C_1im][OAc]$	100.0 ± 0.0	91.9 ± 1.2
1-Butyl-3-methylimidazolium methyl sulfate	$[C_4C_1im][MeSO_4]$	25.9 ± 1.0	0
1-Butyl-3-methylimidazolium methanesulfonate	$[C_4C_1im][MeSO_3]$	32.1 ± 1.2	2.6 ± 0.1
1-Ethyl-3-methylimidazolium hydrogen sulfate	$[C_2C_1im][HSO_4]$	11.2 ± 0.3	0.1 ± 0.0
1-Butyl-3-methylimidazolium hydrogen sulfate	$[C_4C_1im][HSO_4]$	6.7 ± 0.4	0.3 ± 0.1
1-Butyl-3-methylimidazolium chloride	$[C_4C_1im]Cl$	0.1 ± 0.0	0
1-Methylimidazolium acetate	$[C_1Him][OAc]$	98.5 ± 0.4	82.4 ± 2.2
1-Methylimidazolium acetate	$[C_1Him][OAc]$ (1 : 2)	98.4 ± 0.4	66.5 ± 0.1
1-Methylimidazolium acetate	$[C_1Him][OAc]$ (2 : 1)	97.5 ± 0.3	59.0 ± 0.3
1-Methylimidazolium chlorozincate	$[C_1Him][ZnCl_3]$	23.0 ± 0.4	0.1 ± 0.0
1-Methylimidazolium triflate	$[C_1Him][OTf]$	9.0 ± 1.2	2.8 ± 0.3
1-Methylimidazolium chloride	$[C_1Him]Cl$	4.9 ± 0.3	0
1-Methylimidazolium hydrogen sulfate	$[C_1Him][HSO_4]$	3.5 ± 0.3	0
1-Methylimidazolium methanesulfonate	$[C_1Him][MeSO_3]$	1.0 ± 0.3	1.5 ± 0.2
Diazabicyclo(4.3.0)non-5-enium acetate	[DBNH][OAc]	100.0 ± 0.0	46.8 ± 0.4
Diazabicyclo(4.3.0)non-5-enium acetate	[DBNH][OAc] (1 : 2)	100.0 ± 0.0	7.1 ± 0.2
Diazabicyclo(4.3.0)non-5-enium acetate	[DBNH][OAc] (2 : 1)	98.4 ± 0.0	9.2 ± 0.2
Diazabicyclo(4.3.0)non-5-enium methanesulfonate	$[DBNH][MeSO_3]$	16.1 ± 1.0	0.2 ± 0.1
Diazabicyclo(4.3.0)non-5-enium hydrogen sulfate	$[DBNH][HSO_4]$	12.3 ± 0.1	0.1 ± 0.0
Diazabicyclo(4.3.0)non-5-enium chloride	[DBNH]Cl	11.6 ± 1.1	0
1-Methylimidazole		98.4 ± 0.6	92.5 ± 3.5
Diazabicyclo(4.3.0)non-5-ene		100.0 ± 0.0	16.3 ± 4.4
Acetic acid		62 ± 13	52 ± 12
Water (deionised)		0	0

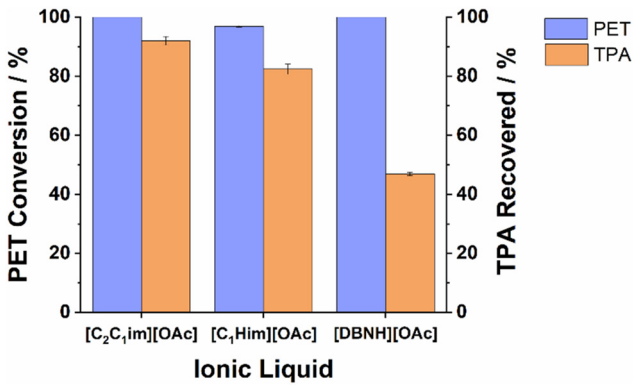

Fig. 5 Conversion and recovered crude TPA yield obtained with various acetate ionic liquids. PET was hydrolysed at 180 °C for 3 h in the presence of 15 wt% water, with a PET loading of 5%.

water, demonstrating the need for using a catalyst or catalytically active solvent. Successful conversion of PET with 1-methylimidazole and DBN shows that the unprotonated base could play a role in promoting PET depolymerisation.[41,42] 1-Methylimidazole is a known catalyst for ester hydrolysis and transesterifications *via* formation of an activated intermediate.[46,47]

PET hydrolysis in components of protic acetate ILs. A high crude yield upon acidification was obtained for 1-methylimidazole (93%), similar to the yield obtained with $[C_2C_1im][OAc]$ (92%), while the crude TPA yield for DBN was low (16%), mirroring the low yield obtained for [DBNH][OAc]. The low yield could be due to hydrolytic decomposition of both DBN and [DBNH][OAc] at 180 °C, as suggested by the ^{1}H-NMR spectrum of [DBNH][OAc] after heating under the reaction conditions (Fig. S25, Table S2).[48,49] The hydrolytic decomposition of DBN and [DBNH][OAc] uses up water, potentially reducing the amount water available for hydrolysis, while the decomposition product, 3-(aminopropyl)-2-pyrrolidone, contains a primary amine that can react with TPA or acetic acid to form amide bonds (Fig. S26).

Acetic acid generated a lower and more variable PET conversion (~62 ± 13%), with a similar crude TPA yield (~52 ± 12%). It is unclear why the standard errors for the measurements in acetic acid were large. A control experiment weighing the samples showed that solvent losses were not responsible for the variation in yield.

PET hydrolysis in non-acetate ILs. PET conversion was low in the non-acetate ILs, including the ones containing the chloride anion (0.1–11%), which was surprising, as $[C_4C_1im]Cl$ had been reported as an effective hydrolysis solvent by Liu *et al.*[36] We repeated the experiment with $[C_4C_1im]Cl$ multiple times, including with the addition of HCl in various amounts based on the hypothesis that the IL used in the previous study may have contained acid impurities, but were unable to reproduce the literature results. The PET conversion could instead perhaps be due to residual alkylimidazole, which our study shows promotes PET hydrolysis.

Low PET conversion was also observed for the methanesulfonate, methyl sulfate, hydrogen sulfate, triflate and chlorozincate ILs. It has been reported that 1-butyl-3-methylimidazolium chlorozincate, $[C_4C_1im][ZnCl_3]$, and 1-allyl-3-methylimidazolium chlorozincate, $[AllC_1im][ZnCl_3]$, catalyse the transesterification of PET with EG with high conversions

(98% and 100%, respectively) and yield BHET as the major product.[50,51] The results for the PET hydrolysis with a chlorozincate IL demonstrates that ILs effective in catalysing PET glycolysis do not necessarily work for PET hydrolysis.

Effect of the acid-to-base ratio in protic acetate ILs. Since protic ILs are made by combining an acid and an amine through simple mixing, it is easy to vary the ratio of both components, which can be expressed as the molar acid-to-base ratio (ABR). The ABR is particularly interesting for protic ILs formed with acetic acid, which are known for incomplete proton transfer from the acid to the amine. [C_1Him][OAc] has been described as a pseudo-protic IL due to substantial quantities of acetic acid and methylimidazole being present in the liquid.[52,53] Hence, molar ABRs other than 1 : 1 were explored for PET hydrolysis with [C_1Him][OAc] and [DBNH][OAc], one with a 50 mol% excess amine and one with 50 mol% excess acetic acid, while all other reaction parameters remained the same. Fig. 6 shows that PET conversion was high for all investigated ABRs, while the crude TPA yield was the highest for the 1 : 1 ABR for both ILs, demonstrating the importance of ABR as an additional reaction and process parameter for protic ILs.

It is currently unclear why the equimolar stoichiometry achieved the best crude product yield for the protic ILs; however, the solvent composition likely affects the hydrogen bonding network and proton transfer equilibrium,[54] which would influence the catalysis in the solvent. Variation of the ABR should be investigated more thoroughly going forward.

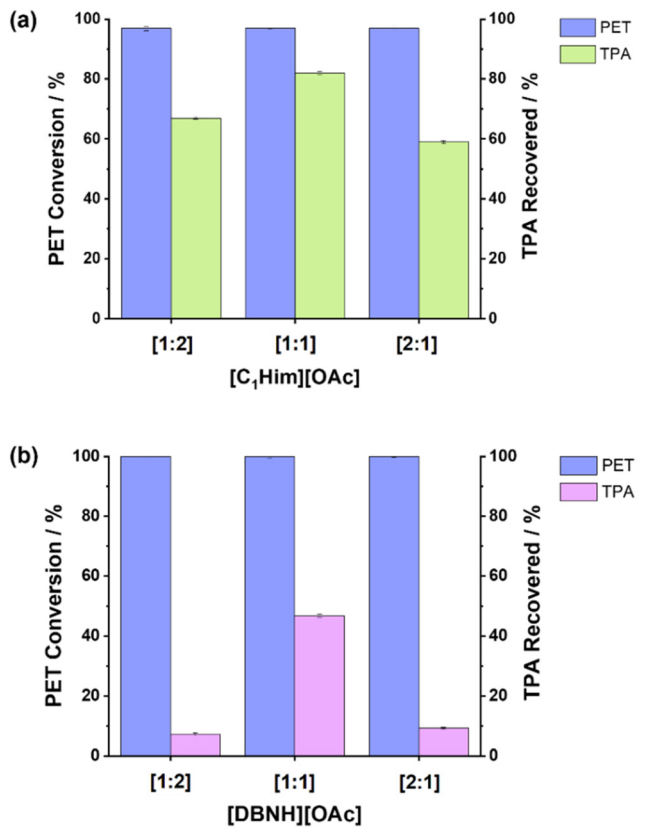

Fig. 6 Effect of changing the ABR (mol : mol) in the protic acetate ILs on PET conversion and crude TPA yield. (a) [C_1Him][OAc] and (b) [DBNH][OAc].

Characterisation of crude TPA recovered from acetate ILs and protic IL precursors

^{1}H-NMR spectra of the crude precipitates (*e.g.* Fig. 4 and Fig. S27) show that the majority of the isolated precipitate was TPA, identified by a singlet peak at 8.0 ppm. The ^{1}H-NMR spectra (Fig. 4 and Fig. S28) also indicate the presence of other compounds with aromatic (7.2–9.0 ppm) and aliphatic signals (0.1–5.0 ppm). These are likely depolymerisation products where TPA is esterified with EG (such as the dimers and trimers), or they may be due to the IL cation. Commercial TPA (Fig. S29) also contained impurities that gave ^{1}H-NMR signals (7.8 and 8.2 ppm), which could be the *ortho*- and *meta*-dicarboxylic acids. Acetic acid (1.9 ppm) was also found in the precipitates generated with acetate ILs and with acetic acid. The amount of acetic acid present in the crude product varied between 0.2 and 3.2 wt% of the crude TPA (Table S3).

While ^{1}H-NMR spectroscopy can be used to detect and quantify TPA, EG, and acetic acid, HPLC is a more precise technique for quantification, as it separates TPA from other similar products. Hence, this study employed HPLC to analyse selected samples, with the method development discussed in the SI, and data on sample purity shown in Fig. 7 and Table S3.

This study shows product purity substantially varied with solvent composition. The purest TPA product (98 wt%) was obtained with [C_1Him][OAc] with a 1 : 2 ABR, followed by the benchmark IL [C_2C_1im][OAc] (92 wt%). Use of acetic acid and 1-methylimidazole also generated high TPA purities (>90%). For the acetate ILs with 1 : 1 stoichiometry, TPA purity followed the same trend as the crude TPA yield ([C_2C_1im][OAc] > [C_1Him][OAc] > [DBNH][OAc]). To meet the requirements for

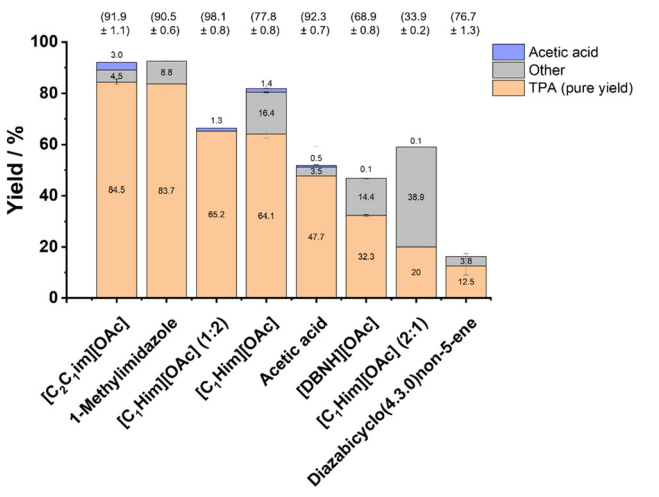

Fig. 7 Pure yield of TPA, adjusted from recovered crude yield and purity (wt%) determined *via* HPLC. Acetic acid content calculated *via* ^{1}H-NMR spectroscopy. TPA purity (wt%) determined by HPLC is shown in brackets above.

polymer-grade TPA (>99%),[55] the crude TPA could be purified *via* crystallisation, as performed in the Amoco process.[56]

The pure TPA yield was determined by combining TPA purity with the crude TPA yield. The highest pure TPA yield was obtained with [C_2C_1im][OAc] (85%) and 1-methylimidazole (84%), while the lowest pure yields were obtained with [DBNH][OAc] and DBN (32% and 13%), which is likely associated with the decomposition of [DBNH][OAc] and DBN (Fig. S26). The decomposition and reactivity of the decomposition product suggest that the performance of the DBN-based IL may not be improved meaningfully with further optimisation. While the equimolar composition of [C_1Him][OAc] yielded the highest crude TPA yield, the pure TPA yield obtained with the excess acid composition was similar (65% and 64%, respectively), further demonstrating the importance of ABR as a reaction parameter.

The HPLC analysis detected up to 22 additional compounds in the isolated crude TPA (Fig. S30). Among them were the partially hydrolysed BHET and HETA products (Fig. S31), which were identified by mass spectrometry. 20 compounds remained unidentified due to the inability to obtain mass spectra with the LC-MS; however, it is likely that they include incompletely hydrolysed PET fragments, such as dimers, trimers and oligomers, which requires further investigation. Comparison of TPA purities determined by mass with the ones obtained by peak area confirmed that a significant proportion of impurities was not detected when employing HPLC-UV-vis analysis (Table S3), which is limited to compounds that are resolved by the eluent and column combination and are UV active. The difference between mass and area purity was particularly high for precipitates generated with [DBNH][OAc] (Δ = −13%), DBN (Δ = −12%) and [C_1Him][OAc] 2 : 1 (Δ = −18%), which also generated the lowest TPA yields (crude and pure). Overall, the 1 : 1 and the excess acid composition of [C_1Him][OAc] resulted in the highest pure TPA yield for protic ILs using the screening conditions, suggesting that these solvents may be preferable.

Solubility of TPA in IL–water mixtures

It was hypothesised that effective PET hydrolysis in IL–water mixtures may be linked to high TPA solubility, as removing the product from solid PET into the liquid phase could promote the hydrolysis reaction. Hence, monomer solubility was qualitatively observed at 5 wt% TPA loading for the IL–water mixtures investigated in this study (Table 2). Visual assessments were converted into the categories yes/no/partially. TPA solubility was found to be strongly anion dependent. All ILs with the acetate anion completely dissolved 5 wt% TPA at 25 °C and 180 °C, which is ascribed to the relatively high pK_a of the acetate anion (4.8), leading to deprotonation of TPA (pK_{a1} 3.5) (Fig. 8), including the IL solvents with excess acid and amine. TPA was also highly soluble in the presence of 1-methylimidazole and DBN, which can also be rationalised by the high pK_as of these amines.[41,42,57] TPA was not notably soluble in the acetic acid–water mixture and deionised water.

Full or partial solubilisation of 5 wt% TPA was observed for certain ILs whose anion has a lower pK_a than that of TPA, for example 1-methylimidazolium chloride, [C_1Him]Cl, [C_4C_1im]Cl and diazabicyclo(4.3.0)non-5-enium chloride, [DBNH]Cl. This is ascribed to the anion being a strong hydrogen bond acceptor (Kamlet–Taft β parameter = 0.83), as shown in Fig. 9. Solubility appeared to be temperature-dependent for these ILs, with better solubility observed at the screening reaction temperature (180 °C).

A substantial cation effect was observed for the ILs with chloride and methanesulfonate anions (Fig. 10). For methanesulfonate ILs, 5 wt% TPA was insoluble at 25 °C in protic 1-methylimidazolum methanesulfonate, [C_1Him][$MeSO_3$], completely soluble in aqueous diazabicyclo(4.3.0)non-5-enium methanesulfonate, [DBNH][$MeSO_3$], and partially soluble in aprotic 1-butyl-3-methylimidazolium methanesulfonate, [C_4C_1im][$MeSO_3$]. It is unclear why the methanesulfonate ILs are subject to a stronger cation effect than the other ILs; the lower pK_a of methanesulfonic acid and the relatively high hydrogen bond basicity (β = 0.77) of the methanesulfonate anion may be playing a role.

5 wt% TPA was not soluble in ILs with a low hydrogen bond acceptor strength, including $[OTf]^-$ and $[ZnCl_3]^-$, nor the ILs with acidic anion and intermediate hydrogen bond basicity, [C_1Him][HSO_4], [C_4C_1im][HSO_4] and diazabicyclo(4.3.0)non-5-enium hydrogen sulfate, [DBNH][HSO_4]. This could be due to the acidic anion favouring TPA protonation and hence formation of crystallised TPA. However, 1-butyl-3-methylimidazolium methyl sulfate, [C_4C_1im][$MeSO_4$], whose anion

Table 2 Qualitative assessment of TPA solubility in the ILs and selected molecular solvents with 15 wt% water. IL solutions containing 5 wt% TPA were heated at 180 °C for 3 h

		Temperature	
		25 °C	180 °C
Methylimidazolium	[C_1Him][OAc]	Y	Y
	[C_1Him][OAc] excess AcOH	Y	Y
	[C_1Him][OAc] excess C_1im	Y	Y
	[C_1Him]Cl	Partially	Y
	[C_1Him][$MeSO_3$]	N	Partially
	[C_1Him][HSO_4]	N	N
	[C_1Him][OTf]	N	N
	[C_1Him][$ZnCl_3$]	N	N
Diazabicyclo(4.3.0) non-5-enium	[DBNH][OAc]	Y	Y
	[DBNH][OAc] excess AcOH	Y	Y
	[DBNH][OAc] excess DBN	Y	Y
	[DBNH]Cl	N	Partially
	[DBNH][$MeSO_3$]	Y	Y
	[DBNH][HSO_4]	N	N
Dialkylimidazolium	[C_2C_1im][OAc]	Y	Y
	[C_2C_1im][HSO_4]	N	N
	[C_4C_1im][OAc]	Y	Y
	[C_4C_1im]Cl	N	Partially
	[C_4C_1im][$MeSO_3$]	Partially	Y
	[C_4C_1im][HSO_4]	N	N
	[C_4C_1im][$MeSO_4$]	N	Partially
Molecular solvents	Acetic acid	N	N
	1-Methylimidazole	Y	Y
	Diazabicyclo(4.3.0) non-5-ene	Y	Y
	De-ionised water	N	N
	Ethylene glycol	N	N

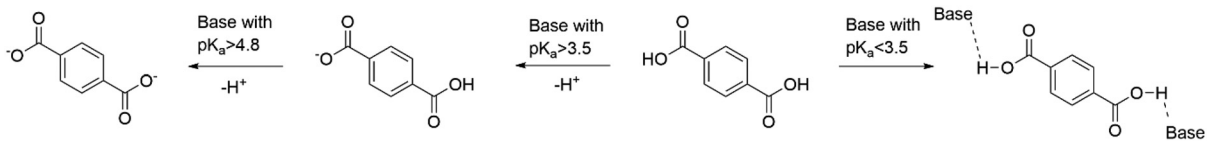

Fig. 8 Interaction of terephthalic acid with Brønsted bases of different strengths. Bases that are not strong enough to deprotonate the carboxylic acid groups may coordinate to TPA through hydrogen bonding.

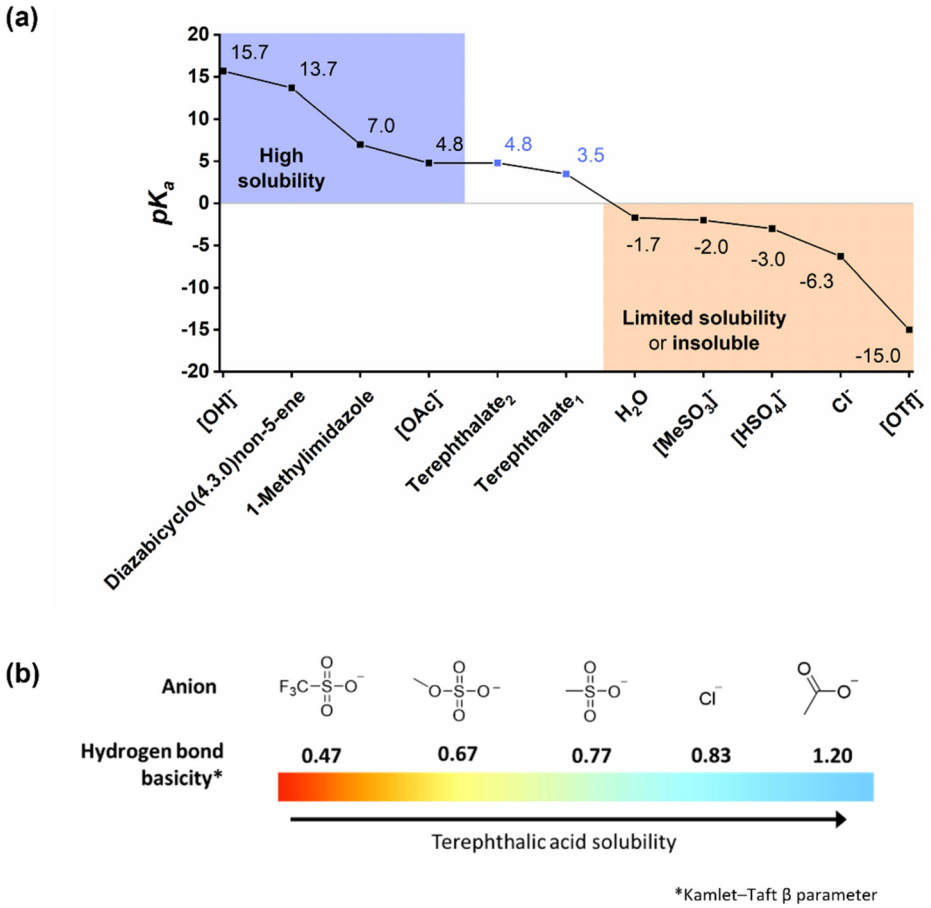

Fig. 9 (a) Relationship between pK_a of the corresponding acid of the IL or molecular solvent used in this study and TPA solubility. TPA exhibits high solubility in Brønsted basic solvents with a high pK_a by generating terephthalate (TPA^{2-}) salts. (b) Relationship between the Kamlet–Taft β parameter of ILs[58] used in this study and TPA solubility. Solubility in solvents with lower pK_a is nuanced and affected by the ability to form strong hydrogen bonds with TPA, of which the Kamlet–Taft β parameter is an indicator of.

has a similar Kamlet–Taft β parameter without the acidity, did not promote TPA solubility at 25 °C, while only partial solubility was observed at 180 °C, suggesting that the hydrogen bonding of sulfate anions is generally insufficient. It is possible that transesterification and hydrolysis involving the methyl sulfate anion occur at 180 °C. Some of the qualitative TPA solubilities reported here are in good agreement with quantitative TPA solubilities reported in the literature for water-free ILs.[59] The solubility of TPA in anhydrous ILs was reported as 25 wt%, 10 wt% and 0 wt% for [C_1Him][OAc], [C_1Him]Cl and [C_1Him][HSO_4], respectively.[59]

Fig. 11 suggests a correlation between TPA solubility and PET conversion; however, notable exceptions include [C_1Him]Cl, [DBNH][$MeSO_3$] and [C_4C_1im][$MeSO_3$], which demonstrated substantial TPA solubility yet poor PET conversion (≤26%). At the same time, acetic acid provided good PET conversion despite its low TPA solubility.

Overall, it was observed that TPA solubility increased with the hydrogen bonding strength of the IL anion and the pK_a of the anion's corresponding acid (Fig. 9). The observations suggest that the anion's hydrogen bond acceptor strength needs to be $\beta > 0.67$ to achieve good TPA solubility or the pK_a

(a)

25 °C	$[OAc]^-$	Cl^-	$[MeSO_3]^-$	$[HSO_4]^-$	$[OTf]^-$
$[C_1Him]^+$	Y	P	N	N	N
$[DBNH]^+$	Y	N	Y	N	
$[C_nC_1im]^+$	Y	N	P	N	

(b)

180 °C	$[OAc]^-$	Cl^-	$[MeSO_3]^-$	$[HSO_4]^-$	$[OTf]^-$
$[C_1Him]^+$	Y	Y	P	N	N
$[DBNH]^+$	Y	P	Y	N	
$[C_nC_1im]^+$	Y	P	Y	N	

Fig. 10 Solubility of TPA in ILs with 15% water shown as a matrix (a) at 25 °C and (b) at 180 °C. ILs ordered according to the Kamlet–Taft hydrogen bond acceptor strength (high to low from left to right).

of the corresponding acid of the anion needs to exceed the pK_{a1} of TPA. Incomplete proton transfer from acid to amine for some protic ILs may also enhance TPA solubility, with the unprotonated amine promoting solubility of the dicarboxylic acid through TPA deprotonation.

PET depolymerisation mechanism in IL–water mixtures

Using the data collected in this study, general features of the depolymerisation mechanism in IL–water mixtures can be discussed. The rate of organic reactions is determined by electronic and steric factors and mass transport. Since PET is insoluble in the IL–water mixtures, PET hydrolysis requires the cleavage of ester linkages at the solid–liquid interface. Formation of cracks confirms that depolymerisation occurs at the surface of PET particles,[16,51,60] and the shrinking-core kinetic model is often assumed.[17,18] Reactions at the solid–liquid interface are often slowed down due to mass transfer limitations, especially if the viscosity is high; however, differences in viscosity do not seem to explain the large variation in the observed PET conversion and TPA yield.

Ester hydrolysis is known to proceed *via* a tetrahedral intermediate (Fig. 12),[61] and its formation can be catalysed by acid or base. It is proposed that the reactive IL solvents enable a base catalysed mechanism, as the anion (acetate) can deprotonate water *via* an equilibrium, generating hydroxide ions which are strong nucleophiles. Hydroxide ions can also be generated *via* an equilibrium involving water and the amines, which could explain why 1-methylimidazole and DBN–water mixtures achieved high PET conversion. In addition, deprotonation of TPA drives conversion by shifting the equilibrium to the product side, which may also promote PET conversion.

It is proposed that of the two protic acetate ILs, only [C_1Him][OAc] supplies noticeable quantities of amine without decomposition,[54] due to the relatively low pK_a difference between amine and acetic acid ($\Delta pK_a < 3$). The high PET conversion for acetate ILs, 1-methylimidazole and DBN can be explained by the (irreversible) deprotonation of TPA and carboxylic acid end groups of short oligomers; hence their reactivity is well-correlated with solubility. The data show that all tested ILs reduce the activation energy compared to water, which is a weak nucleophile. However, they require higher temperatures (at the same reaction time) compared to aqueous solutions of NaOH, due to the lower OH^- concentration.

The cation has been assigned a stabilising role for the tetrahedral intermediate;[18,38,62,63] however, our data do not provide evidence for specific interactions, especially since a number of Brønsted acidic sites are present, such as on the cation, hydronium ions and acetic acid. Generally, activation of the carbonyl group is more important for the acid catalysed ester hydrolysis mechanism than for the base catalysed mechanism. In support of the proposed mechanism, high proton affinity (correlated to the Kamlet–Taft parameter, β) of ILs was reported to

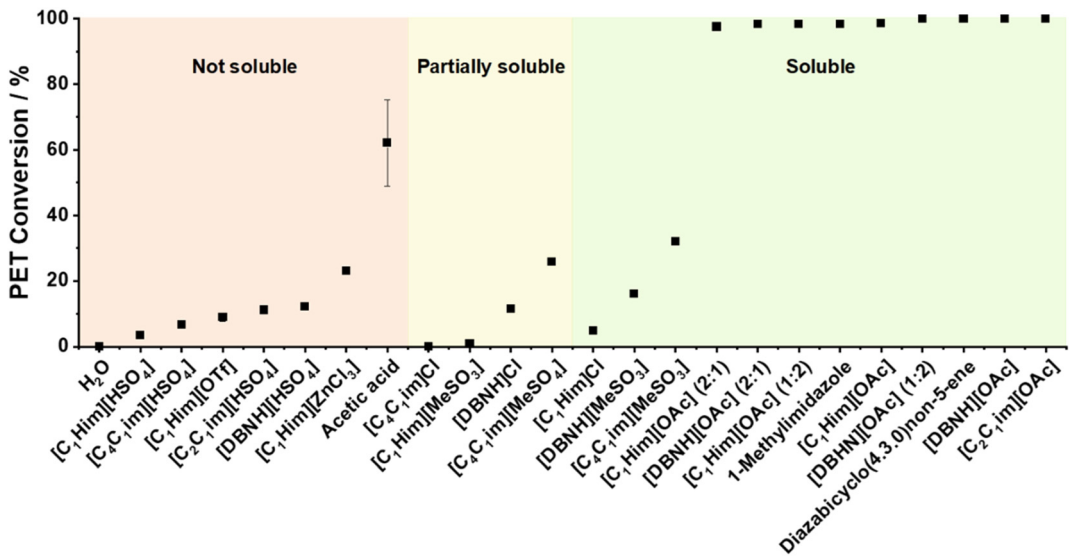

Fig. 11 PET conversion in ILs or molecular solvents at 180 °C after 3 h with 15 wt% H_2O present, categorised according to solubility of 5 wt% TPA in the aqueous solvent mixtures.

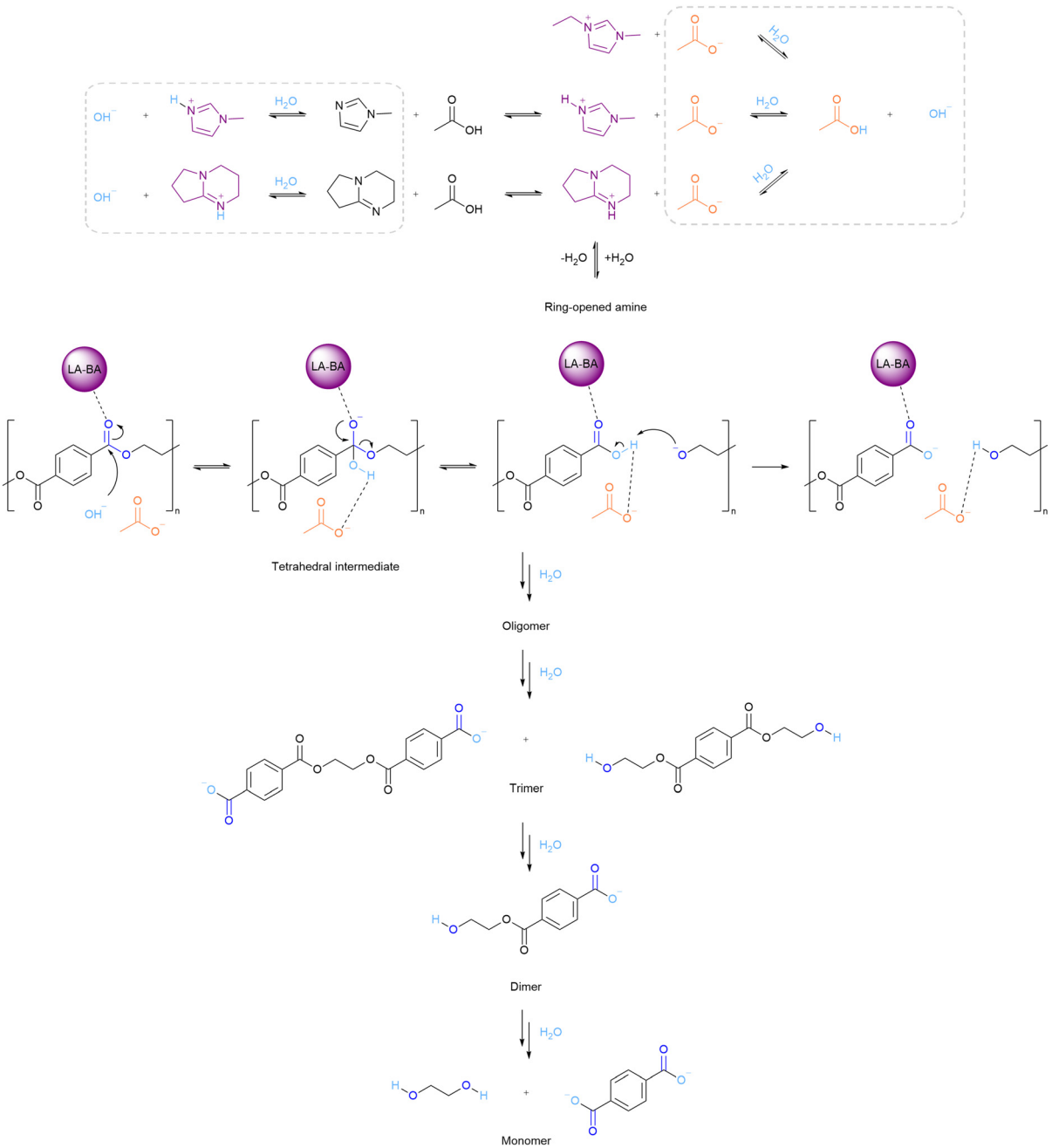

Fig. 12 Proposed IL-catalysed PET hydrolysis reaction mechanism using aprotic and protic acetate ILs.

lower the reaction rate of esterification (the reverse reaction of hydrolysis).[64] It is proposed that in acetic acid–water mixtures, the acid catalysed ester hydrolysis mechanism is applicable. These mechanistic considerations are suggestions and require deeper investigation.

Consideration of process aspects, including solvent cost and hazards

Solvent recovery and cost are key for developing viable solvent-based chemical processes.[65] IL stability is a concern in PET depolymerisation due to the elevated temperatures required to achieve good PET conversions and TPA yields at an acceptable reaction rate. Solvent and reagent stability provide an upper limit for reaction temperatures. Fig. 13 depicts a colour change for the $[C_2C_1im][OAc]$–water mixture, which started as a colourless solution and gradually turned dark brown. The discolouration was accompanied by the appearance of at least four new peaks (δ = 7.6, 7.2, 6.9 and 3.6 ppm) in the ^{1}H-NMR spectrum at ~2 mol% (Fig. S32 and Table S4), which suggests dealkylation of 1-ethyl-3-methylimidazolium by acetate to 1-alkylimidazoles and esters of acetic acid. This was expected, given the low stability of anhydrous $[C_2C_1im][OAc]$ at 180 °C.[66,67]

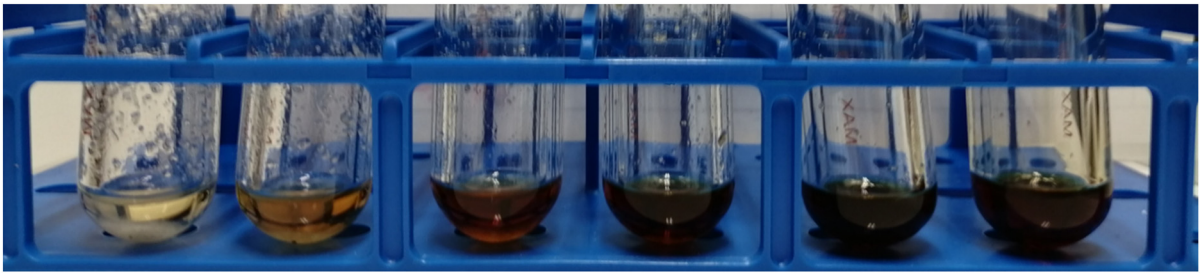

Fig. 13 Samples containing $[C_2C_1im][OAc]$ with 15 wt% water and 5% shredded bottle PET heated at 180 °C as a function of time. Hydrolysis duration from 0.5 h (left) to 3 h (right) in 0.5 h increments.

Interestingly, this decomposition does not necessarily lower the IL's performance in this application, given that 1-methylimidazole also promoted PET hydrolysis. Varying degrees of discolouration were observed for the other ILs after PET depolymerisation (Fig. S33), except for $[C_4C_1im][MeSO_3]$. The ^{1}H-NMR spectrum of [DBNH][OAc], after applying the screening conditions, was examined and revealed the appearance of seven new peaks, suggesting again the presence of the ring-opened hydrolysis product (Fig. S25 and Table S2).[49] This decomposition may be linked to the lower performance of the [DBNH][OAc]–water mixture, as discussed earlier. In other cases, notable decomposition products were not observed in the ^{1}H-NMR spectra, despite the solvent becoming strongly coloured during heating, for example, the $[C_1Him][OAc]$–water mixture (Fig. S34 and Table S5). A more thorough and quantitative study of the link between PET hydrolysis performance and IL stability under process conditions should be carried out in the future.

$[C_1Him][OAc]$ emerged from this study as a promising candidate, with good performance (PET conversion, TPA yield and purity) and stability. Hence, we estimated the cost of the IL using a process model developed by Chen *et al.*[68] and compared it to the cost of the aprotic $[C_2C_1im][OAc]$ (Table 3), which requires a more complex synthesis involving alkylation of the alkylimidazole and ion exchange. Details of the calculations can be found in the SI (Table S6). The cost estimate reveals that the production cost for the $[C_1Him][OAc]$–water mixture is <10% of the cost of $[C_2C_1im][OAc]$, whose synthesis was modelled as an alkylation of methylimidazole with ethyl chloride, followed by ion exchange.[69] The model assumes that solvent costs are dominated by input cost for protic ILs at scale.[68] The cost differences are due to additional synthetic steps needed for aprotic ILs.

In our cost estimate, excess acid in the IL reduced the solvent cost, due to acetic acid being the cheaper component. A higher water content for hydrolysis may also reduce the cost further; hence increasing the water content should be investigated further. The estimated cost of the $[C_1Him][OAc]$–water compositions is in the range of common organic solvents, such as acetone and ethyl acetate (1.30–1.40 $ per kg).[68]

When designing a sustainable chemical process, solvent hazards should also be considered, although use of a hazardous solvent can result in an overall more sustainable chemical process.[71] ILs are currently produced at a small scale and hence limited commercial toxicity data are available. For example, the $[OTf]^-$ anion is undesirable, as it is fluorinated and hence likely persistent in the environment, while the Zn-containing anion is undesirable as Zn is a toxic heavy metal. 1-Methylimidazole has moderate toxicity, however, it has recently been classified as a teratogen under European REACH legislation. DBN is imported in the EU <1 tonne and hence does not have a REACH dossier. It is noted for its corrosiveness which is typical of amines. Acetic acid is also corrosive in its concentrated form and is classified as a flammable liquid but has otherwise low toxicity and is readily biobased. Decomposition products may modulate the solvent toxicity profile. The chemical hazards of the solvent need to be balanced with the benefit of a potential chemical recycling process and compared to the hazards and environmental impact of TPA and EG production from new (fossil) feedstocks.

The addition of an acid to precipitate the TPA from solution as carried out here changes the composition of the IL,[23,57] making chemical PET recycling as carried out in this screening study uneconomical, while increasing environmental burdens by requiring fresh solvent. Recovery of TPA by antisolvent crystallisation (with water) and EG by distillation would be prefer-

Table 3 Estimated solvent cost of $[C_2C_1][OAc]$–water and $[C_1Him][OAc]$–water mixtures used in this study. Cost estimate for anhydrous $[C_2C_1im][OAc]$ ($35 per kg) adapted from Morales,[69] and utility cost for process water from Turton *et al.*[70]

Solvent	Cost of amine ($ per kg of IL)	Cost of acid ($ per kg of IL)	Cost of water ($ per kg)	Solvent cost ($ per kg of IL–water mixture)
$[C_2C_1im][OAc]$ + 15% water	N/A	N/A		$29.8
$[C_1Him][OAc]$ + 15% water	$1.84	$0.27	$1.77 × 10^{-4}	$2.11
$[C_1Him][OAc]$ (1 : 2) + 15% water	$1.29	$0.38		$1.67

able and will be investigated for the lead solvent going forward.

Conclusions

This screening study found that hydrolysis of shredded bottle PET in IL–water mixtures strongly depends on anion selection. PET hydrolysis with the aprotic IL, $[C_2C_1im][OAc]$, yielded screening conditions (180 °C, 3 h, 15 wt% H_2O, 5% PET loading), which were successfully used to evaluate a library of aprotic and protic ILs. ILs with acetate anions gave the highest PET conversion and the highest isolated TPA yields (after dilution and acidification), regardless of whether they were protic or aprotic ILs. It was also found that measuring the percentage yield of the precipitated product typically overestimates TPA yield, as other hydrolysis products and solvent impurities are present in the crystallised product, shown by ^{1}H-NMR spectroscopy and HPLC. It is hence strongly recommended that TPA purity is determined quantitatively to better evaluate solvent performance.

The pseudo-protic IL, $[C_1Him][OAc]$, performed well in the screening, enabling high PET conversion (99%) and crude TPA yield (82%), and good TPA purity (78%) at acceptable temperatures, with 10 times lower solvent cost than the aprotic $[C_2C_1im][OAc]$, which is encouraging for further study and process development. The IL–water mixtures based on $[C_1Him][OAc]$ at 1 : 1 and 1 : 2 ABRs generated similar TPA yields, showing that increasing the ABR can help lower solvent cost.

Solubility of TPA could be correlated with the strength of interactions between the carboxylic acid groups in TPA and the anion of the IL, as found for other solutes containing hydroxyl groups such as cellulose or lignin.[39] The pK_a of the IL anion exceeding the pK_a of terephthalate was a strong predictor of TPA solubility. Strong hydrogen bond acceptance could also promote solubilisation of TPA, even if the pK_a of the anion was below the threshold. TPA solubility generally correlated with PET conversion, but some IL solvents with notable TPA solubility exhibited low PET conversion under the screening conditions. Based on the available data, it is proposed that acetate ILs promote depolymerisation of PET *via* the base catalysed ester hydrolysis mechanism, driven by TPA deprotonation. Based on the promising results observed for $[C_1Him][OAc]$–water mixtures, a waste-free recovery method for the monomers TPA and EG should be developed, which is underway in our laboratory.

Author contributions

M. Y. S.: investigation, writing – original draft, formal analysis and visualisation. H. L. J.: methodology, investigation, formal data analysis and visualisation. P. B.: methodology and investigation. P. F.: conceptualisation, funding acquisition and supervision. J. P. H.: conceptualisation, funding acquisition and supervision. A. B.-T.: conceptualisation, funding acquisition, supervision and project administration. All authors contributed to writing – reviewing and editing.

Conflicts of interest

The authors have no conflicts to declare.

Data availability

Data supporting this article have been included as part of the SI file, which contains details relating to IL synthesis, HPLC method development, characterisation of the isolated TPA and IL solutions after use and details for solvent cost estimations. See DOI: **https://doi.org/10.1039/d5gc02409a**.

Acknowledgements

We acknowledge funding of the work *via* EP/S025456/1, NE/W503198/1, EP/R513052/1 and EP/S023232/1. The authors thank Ruhi Patel and Reeya Patel for assistance in preliminary experiments, Tom Welton for advice, and Chris Roberts from the Centre for Rapid Online Analysis of Reactions (ROAR) facility for assisting with the development of the HPLC method, funded *via* EP/R008825/1 and EP/V029037/1.

References

1 R. Geyer, J. R. Jambeck and K. L. Law, *Sci. Adv.*, 2017, **3**, e1700782.
2 A. Rahimi and J. M. García, *Nat. Rev. Chem.*, 2017, **1**, 0046.
3 K. Kaiser, M. Schmid and M. Schlummer, *Recycling*, 2017, **3**, 1.
4 *Plastics - the Facts* 2022, Plastics Europe, 2022.
5 D. K. Schneiderman and M. A. Hillmyer, *Macromolecules*, 2017, **50**, 3733–3749.
6 G. P. Karayannidis and D. S. Achilias, *Macromol. Mater. Eng.*, 2007, **292**, 128–146.
7 A. C. Castillo, M. Malakkal, P. Bexis and K. Brophy, *Enabling a greener plastic future through molecular science*, Imprerial College London, Institute for Molecular Sciences and Engineering, 2020.
8 M. Babaei, M. Jalilian and K. Shahbaz, *J. Environ. Chem. Eng.*, 2024, **12**, 112507.
9 G. W. Coates and Y. D. Y. L. Getzler, *Nat. Rev. Mater.*, 2020, **5**, 501–516.
10 Y.-H. V. Soong, M. J. Sobkowicz and D. Xie, *Bioengineering*, 2022, **9**, 98.
11 K. Ragaert, L. Delva and K. Van Geem, *Waste Manage.*, 2017, **69**, 24–58.
12 B. Geyer, G. Lorenz and A. Kandelbauer, *eXPRESS Polym. Lett.*, 2016, **10**, 559–586.
13 Y. Peng, J. Yang, C. Deng, J. Deng, L. Shen and Y. Fu, *Nat. Commun.*, 2023, **14**, 3249.

14 T. Uekert, J. S. DesVeaux, A. Singh, S. R. Nicholson, P. Lamers, T. Ghosh, J. E. McGeehan, A. C. Carpenter and G. T. Beckham, *Green Chem.*, 2022, **24**, 6531–6543.
15 L. Cottam and R. P. Sheldon, *Nature*, 1965, **205**, 1005–1005.
16 A. M. Al-Sabagh, F. Z. Yehia, A.-M. M. F. Eissa, M. E. Moustafa, G. Eshaq, A.-R. M. Rabie and A. E. ElMetwally, *Ind. Eng. Chem. Res.*, 2014, **53**, 18443–18451.
17 Y. Liu, X. Yao, H. Yao, Q. Zhou, J. Xin, X. Lu and S. Zhang, *Green Chem.*, 2020, **22**, 3122–3131.
18 R. Zhang, X. Zheng, X. Yao, K. Song, Q. Zhou, C. Shi, J. Xu, Y. Li, J. Xin, I. E.-T. El Sayed and X. Lu, *Ind. Eng. Chem. Res.*, 2023, **62**, 11851–11861.
19 G. Grause, J. Sutton, A. P. Dove, N. A. Mitchell and J. Wood, *Cryst. Growth Des.*, 2024, **24**, 7306–7321.
20 T. Wang, X. Gong, C. Shen, G. Yu and X. Chen, *Polym. Degrad. Stab.*, 2021, **190**, 109601.
21 C. N. Onwucha, C. O. Ehi-Eromosele, S. O. Ajayi, M. Schaefer, S. Indris and H. Ehrenberg, *Ind. Eng. Chem. Res.*, 2023, **62**, 6378–6385.
22 S. Ügdüler, K. M. Van Geem, R. Denolf, M. Roosen, N. Mys, K. Ragaert and S. De Meester, *Green Chem.*, 2020, **22**, 5376–5394.
23 O. A. Attallah, M. Azeem, E. Nikolaivits, E. Topakas and M. B. Fournet, *Polymers*, 2022, **14**, 109.
24 M. Rollo, F. Raffi, E. Rossi, M. Tiecco, E. Martinelli and G. Ciancaleoni, *Chem. Eng. J.*, 2023, **456**, 141092.
25 I. Cano, C. Martin, J. A. Fernandes, R. W. Lodge, J. Dupont, F. A. Casado-Carmona, R. Lucena, S. Cardenas, V. Sans and I. de Pedro, *Appl. Catal., B*, 2020, **260**, 118110.
26 A. M. Al-Sabagh, F. Z. Yehia, A. M. F. Eissa, M. E. Moustafa, G. Eshaq, A. M. Rabie and A. E. ElMetwally, *Polym. Degrad. Stab.*, 2014, **110**, 364–377.
27 T. Wang, C. Shen, G. Yu and X. Chen, *Polym. Degrad. Stab.*, 2022, **203**, 110050.
28 C. Jehanno, I. Flores, A. P. Dove, A. J. Müller, F. Ruipérez and H. Sardon, *Green Chem.*, 2018, **20**, 1205–1212.
29 R. Zhang, X. Zheng, X. Cheng, J. Xu, Y. Li, Q. Zhou, J. Xin, D. Yan and X. Lu, *Materials*, 2024, **17**, 1583.
30 C. Zhu, L. Yang, C. Chen, G. Zeng and W. Jiang, *Phys. Chem. Chem. Phys.*, 2023, **25**, 27936–27941.
31 J. D. Badia, R. Ballesteros-Garrido, A. Gamir-Cobacho, O. Gil-Castell and A. Cháfer, *J. Environ. Chem. Eng.*, 2024, **12**, 113134.
32 N. Liu, Y. S. Ma, K. W. Shu, B. Wu and D. Zhang, *Adv. Mater. Res.*, 2014, **893**, 23–26.
33 R. M. Musale and S. R. Shukla, *J. Text. Inst.*, 2017, **108**, 467–471.
34 C. Dou, H. Choudhary, Z. Wang, N. R. Baral, M. Mohan, R. A. Aguilar, S. Huang, A. Holiday, D. R. Banatao, S. Singh, C. D. Scown, J. D. Keasling, B. A. Simmons and N. Sun, *One Earth*, 2023, **6**, 1576–1590.
35 J. Sun, D. Liu, R. P. Young, A. G. Cruz, N. G. Isern, T. Schuerg, J. R. Cort, B. A. Simmons and S. Singh, *ChemSusChem*, 2018, **11**, 781–792.
36 F. Liu, X. Cui, S. Yu, Z. Li and X. Ge, *J. Appl. Polym. Sci.*, 2009, **114**, 3561–3565.
37 A. S. Amarasekara, J. A. Gonzalez and V. C. Nwankwo, *J. Ionic Liq.*, 2022, **2**, 100021.
38 Z. Zhao, J. Bai, H. Tao, S. Wang, K. Wang, W. Lin, L. Jiang, H. Li and C. Wang, *Green Chem. Eng.*, 2024, DOI: **10.1016/j.gce.2024.12.001**.
39 A. Brandt, J. Grasvik, J. P. Hallett and T. Welton, *Green Chem.*, 2013, **15**, 550–583.
40 A. J. Greer, J. Jacquemin and C. Hardacre, *Molecules*, 2020, **25**, 5207.
41 D. Sanna, V. Ugone, G. Micera, P. Buglyó, L. Bíró and E. Garribba, *Dalton Trans.*, 2017, **46**, 8950–8967.
42 C. Wiles and P. Watts, *Beilstein J. Org. Chem.*, 2011, **7**, 1360–1371.
43 S. Kaiho, A. A. R. Hmayed, K. R. D. Chiaie, J. C. Worch and A. P. Dove, *Macromolecules*, 2022, **55**, 10628–10639.
44 L. Cosimbescu, D. R. Merkel, J. Darsell and G. Petrossian, *Ind. Eng. Chem. Res.*, 2021, **60**, 12792–12797.
45 G. P. Karayannidis, A. P. Chatziavgoustis and D. S. Achilias, *Adv. Polym. Technol.*, 2002, **21**, 250–259.
46 G. O. Andrés, A. M. Granados and R. H. de Rossi, *J. Org. Chem.*, 2001, **66**, 7653–7657.
47 P. A. R. Pires, N. I. Malek, T. C. Teixeira, T. A. Bioni, H. Nawaz and O. A. E. Seoud, *Ind. Crops Prod.*, 2015, **77**, 180–189.
48 F. S. Pereira, D. L. da S. Agostini, R. D. do E. Santo, E. R. deAzevedo, T. J. Bonagamba, A. E. Job and E. R. P. González, *Green Chem.*, 2011, **13**, 2146–2153.
49 A. Parviainen, R. Wahlström, U. Liimatainen, T. Liitiä, S. Rovio, J. K. J. Helminen, U. Hyväkkö, A. W. T. King, A. Suurnäkki and I. Kilpeläinen, *RSC Adv.*, 2015, **5**, 69728–69737.
50 Q. F. Yue, H. G. Yang, M. L. Zhang and X. F. Bai, *Adv. Mater. Sci. Eng.*, 2014, **2014**, 454756.
51 Q. Wang, X. Lu, X. Zhou, M. Zhu, H. He and X. Zhang, *J. Appl. Polym. Sci.*, 2013, **129**, 3574–3581.
52 L. Wylie, M. Kéri, A. Udvardy, O. Hollóczki and B. Kirchner, *ChemSusChem*, 2023, **16**, e202300535.
53 K. Chen, Y. Wang, J. Yao and H. Li, *J. Phys. Chem. B*, 2018, **122**, 309–315.
54 H. Watanabe, N. Arai, H. Jihae, Y. Kawana and Y. Umebayashi, *J. Mol. Liq.*, 2022, **352**, 118705.
55 N. S. Allen, M. Edge, J. Daniels and D. Royall, *Polym. Degrad. Stab.*, 1998, **62**, 373–383.
56 R. A. F. Tomás, J. C. M. Bordado, J. F. P. Gomes and R. J. Sheehan, in *Ullmann's Encyclopedia of Industrial Chemistry*, 2024, pp. 1–17, DOI: **10.1002/14356007.a26_193.pub3**.
57 J. P. Mészáros, W. Kandioller, G. Spengler, A. Prado-Roller, B. K. Keppler and É. A. Enyedy, *Pharmaceutics*, 2023, **15**, 356.
58 M. A. Ab Rani, A. Brant, L. Crowhurst, A. Dolan, M. Lui, N. H. Hassan, J. P. Hallett, P. A. Hunt, H. Niedermeyer, J. M. Perez-Arlandis, M. Schrems, T. Welton and R. Wilding, *Phys. Chem. Chem. Phys.*, 2011, **13**, 16831–16840.
59 K. Matuszek, E. Pankalla, A. Grymel, P. Latos and A. Chrobok, *Molecules*, 2020, **25**, 80.
60 X. Zhou, X. Lu, Q. Wang, M. Zhu and Z. Li, *Pure Appl. Chem.*, 2012, **84**, 789–801.

61 J. Clayden, N. Greeves, S. Warren and P. Wothers, *Organic Chemistry*, Oxford University Press, Oxford, 1st edn, 2001.
62 H. Wang, Z. Li, Y. Liu, X. Zhang and S. Zhang, *Green Chem.*, 2009, **11**, 1568–1575.
63 F. Scé, I. Cano, C. Martin, G. Beobide, Ó. Castillo and I. de Pedro, *New J. Chem.*, 2019, **43**, 3476–3485.
64 T. P. Wells, J. P. Hallett, C. K. Williams and T. Welton, *J. Org. Chem.*, 2008, **73**, 5585–5588.
65 H. Baaqel, I. Díaz, V. Tulus, B. Chachuat, G. Guillén-Gosálbez and J. P. Hallett, *Green Chem.*, 2020, **22**, 3132–3140.
66 J. D. Oxley, T. Prozorov and K. S. Suslick, *J. Am. Chem. Soc.*, 2003, **125**, 11138–11139.
67 M. T. Clough, K. Geyer, P. A. Hunt, J. Mertes and T. Welton, *Phys. Chem. Chem. Phys.*, 2013, **15**, 20480–20495.
68 L. Chen, M. Sharifzadeh, N. Mac Dowell, T. Welton, N. Shah and J. P. Hallett, *Green Chem.*, 2014, **16**, 3098–3106.
69 M. Morales, *Process Design and Sustainability Assessment for Biorefinery Technologies*, ETH, Zurich, 2016, DOI: **10.3929/ethz-a-010797794**.
70 R. Turton, J. A. Shaeiwitz, D. Bhattacharyya and W. B. Whiting, *Analysis, synthesis, and design of chemical processes*, ed. R. Turton, J. A. Shaeiwitz, D. Bhattacharyya and W. B. Whiting Prentice Hall, Boston, 5th edn, 2018.
71 T. Welton, *Proc. R. Soc. A*, 2015, **471**, 20150502.

